

Detailed studies of erosion control geomats using laser Doppler anemometry

D.J. McKay & N. Hytiris

Department of Energy and Environmental Technology, Glasgow Caledonian University, Glasgow, Scotland, UK

P.S. Addison

Department of Civil and Transportation Engineering, Napier University, Edinburgh, Scotland, UK

Keywords: Erosion control, Geomats, Laboratory research, Rolled erosion control products, Testing

ABSTRACT: To date, no detailed analysis of the flow properties over and through turf reinforcement geomats has been undertaken. This paper details an experimental programme of research, initiated by the authors, to allow for the examination of the flow-field at the fluid - geomat - sediment interface. The work discussed herein continues from an earlier study (McKay et al. 1998), and compares the flow profiles through various mattings currently available on the commercial market. By doing so, the first step towards a comprehensive theoretical framework is developed for the flow-field over and within such mats.

1 INTRODUCTION

Geosynthetics in the form of turf reinforcement mattings (TRMs) have become a regularly used form of erosion protection in open channel flows. However, the effect of such mats upon the hydraulic conditions have until recently been unknown. Using a large flume and laser Doppler anemometry (LDA) techniques, the authors have been able to collect detailed velocity and turbulence intensity measurements both within the internal structure of, and above, various commercially available erosion control geosynthetic mattings.

All commercially available mats could easily be grouped into three main categories:

1. Random heat bonded monofilament,
2. Heat bonded geogrid and
3. Stitched geonet

The selection of mats used within this study enabled the above three main methods of mat construction to be studied, so as to provide an overview of the flow characteristics of an average geomat lined channel.

The flow-fields generated by the mats were studied using the LDA system, and the profiles of turbulence and velocity for the flow above and within the mat plotted. These results indicated that the flow characteristics within and above all forms of mat structure investigated produce similar profiles. This prompted the authors to investigate the possibility of using a modified logarithmic law of the wall equation (Eq. 2) for the flow velocity profiles. The log-law equation (Garde et al. 1977, Nezu et al. 1986, Nezu et al. 1993, Yalin 1972) is not applicable within the internal, structural region, of the mat. Hence, this study focuses on the region from the fluid-mat interface to the fluid surface.

2 EXPERIMENTAL SETUP AND CONDITIONS

The experiments discussed herein were all conducted in a 4m long, 0.6m wide tilting flume. The depth of flow was kept at a constant 0.1m by attaining the desired flow rate of 6.0 l/s and using the

flume's adjustable tailgate for depth adjustments. The instantaneous stream-wise velocity component was measured using a 1-D Dantec LDA system (Keogh et al. 1996). This was placed 2m downstream of the inlet tank, situated underneath the flume to enable readings to be taken vertically through the depth of flow. The various synthetic materials used were secured to the flume bed using wire ties and covered its entire floor surface.

2.1 Geosynthetic Mattings

The geomats used in this study covered a wide range of designs (descriptions of which can be found in Table 1 below).

Table 1: A description of the Commercially Available Mats used in the Study

Matting	Nominal Thickness* (mm)	General Description
N ^o . 1	18	Cusped 'egg-box' mesh, heatbonded to a flat base mesh
N ^o . 2	20	3 layers of stitched mesh (central corrugated)
N ^o . 3	18	Open form mat of heatbonded, random polyamide monofilament 'arches'
N ^o . 4	19.5	Flat-backed heatbonded polypropylene mat of random monofilament structure

*Nominal thickness' as from Manufacturers Specifications

All the mats tested here comprised a three-dimensional polymer structure which is designed to provide reinforcement to any turf root system and hence they are often called 'turf reinforcement mats' [TRMs]. In practice the mats are placed so as to provide temporary protection to a bare soil during vegetation growth. Subsequently, they permanently reinforce the full-grown vegetation increasing its erosional resistance. However, these tests were designed to look at a critical stage of design and placement of TRMs, which is during initial placement with little or no filling and no turf growth; where success or failure is dependant only on the mats structural integrity.

3 EXPERIMENTAL RESULTS & ANALYSIS

The flume was set so as to provide a depth of flow of $h = 0.1\text{m}$ at a flow rate $Q = 6\text{ l/s}$. Control tests consisting of runs in the bare channel were undertaken, the results of which can be seen in Figure 1. Figure 1a contains both the experimental and theoretical velocity profiles for the bare flume and figure 1b contains the corresponding turbulence intensities throughout the depth.

Figure 2 shows the results of the mat experiments. These results represent the ensemble averages of multiple tests, which were taken at various locations above the flume bed, so as to give an average measurement of the overall profiles both within and above the mats.

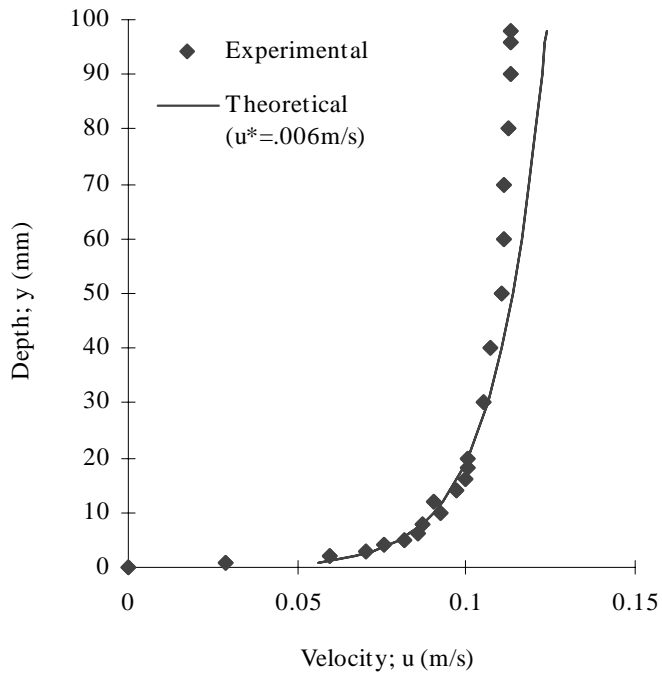


Figure 1a. Velocity profiles

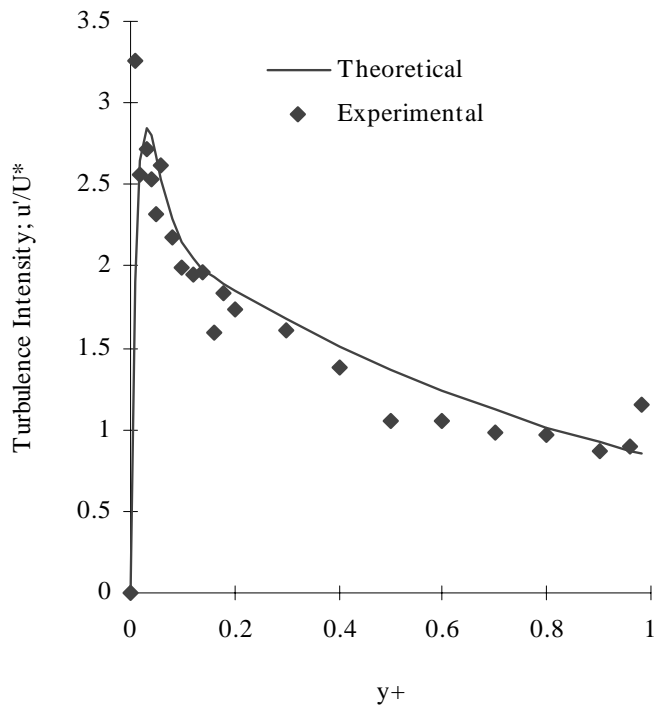


Figure 1b. Turbulence intensity profiles

Figure 1. Bare channel experimental and theoretical profiles

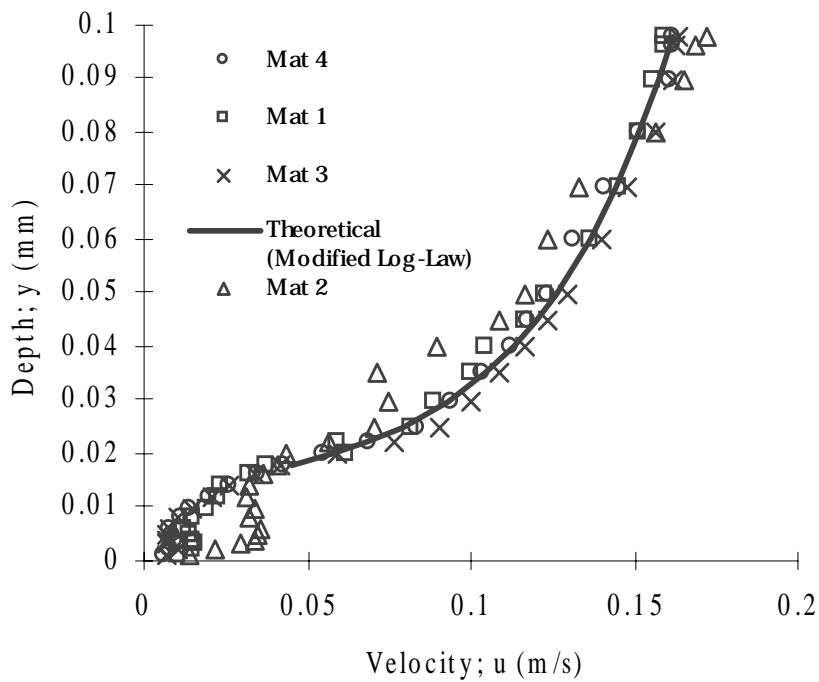


Figure 2a; Velocity Profiles

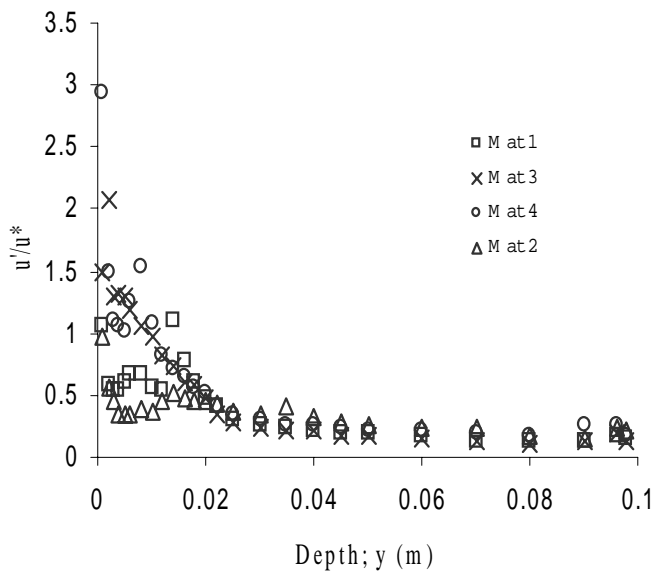


Figure 2b; Turbulence profiles

Figures. 2; Profiles of Mat Lined Channels

All of the mat velocity profiles (Fig. 2a), except mat 2, exhibit a similar form of profile. For these mats, the flow-fields above the mat region show a profile similar to that for a flow rate of ninety-six percent of the overall flow, the remaining four percent of the overall flow being within the mat structure. A gentle transitional gradient of the profile at a location between the depth at the nominal mat thickness to a depth of approximately $y \approx 0.008\text{m}$ can then be seen. Finally occurs a

‘steading’ of the flow velocity down from the $y = 0.008\text{m}$ location to the base level. Mat 2 differs from the other mats by having increased mat region flow, due to its extremely open structure, and by having erroneous points in the upper regions caused by poor structural integrity which allowed the top grid layer to sit well into the main flow region at certain locations.

The profile shapes near to the bed are the result of a ‘virtual bottom’ (Chow 1973) created at a depth high within the mat structure, which reduces the flow rate of that region, compared to a similar zone in a bare channel. The reduction in flow rate in the mat region induces an a reforming of the flow profile to accommodate the lower velocities, at the virtual bottom, while ensuring the flow rates remain constant. The profiles of turbulence intensity also show a great similarity, as can be seen from Figure 2b.

The logarithmic law for open channel flows is given by;

$$\frac{u}{u_*} = \frac{1}{\kappa} \ln y^+ + A \quad [1]$$

Where the shear velocity; u_* , can be estimated from: $u_* = (gRs)^{0.5}$ during normal conditions (R being the hydraulic radius, s the hydraulic gradient and g the acceleration due to gravity).

κ is the Von Karman constant equal to 0.41 under most normal circumstances (but has been noted within the ranges of 0.6-0.16 (Yalin 1972)); y^+ (equal to y/ℓ in rough conditions) is a dimensionless y co-ordinate and A is a constant equal to 8.5 for rough conditions. However, equation 1 will not provide a velocity distribution for a channel lined with geosynthetic mat (as can be seen from Fig. 3) due to the “virtual” bottom created by the mat. Equation 1 is therefore modified to take this into account as follows:

$$\frac{u}{u_*} = \frac{1}{\kappa} \ln \frac{y'}{k_s} + A \quad [2]$$

Here y' equals $y - k_g$ which takes account of the depth from the “virtual” base or zero plane displacement, k_g . From the work completed by the authors, k_g sits between $y = 0.011\text{-}0.017\text{ m}$ for mat thickness’ ranging from $y = 0.018\text{-}0.02\text{m}$. k_s is the bed roughness coefficient. However, due to the complicated nature of the flow physics within the internal mat structure, Equation 2 does not hold within the mat region. Equation 2 was used to produce the logarithmic profile superimposed on Figure 2a.

Turbulence Intensity (TI), for the bare channel, was calculated using Equation 3 (Nezu et al. 1993).

$$\frac{u'}{u_*} = D_u \exp(-\lambda_u \xi) \Gamma + 0.3 y^+ \cdot (1 - \Gamma) \quad [3]$$

Where $D_u = 2.26$, $\lambda_u = 1$ are empirical functions, $\xi \equiv y/h$ and Γ is the damping function, calculated from Equation 4.

$$\Gamma = 1 - \exp\left(-\frac{\xi}{B'}\right) \quad [4]$$

With the damping coefficient; $B' = 0.02$.

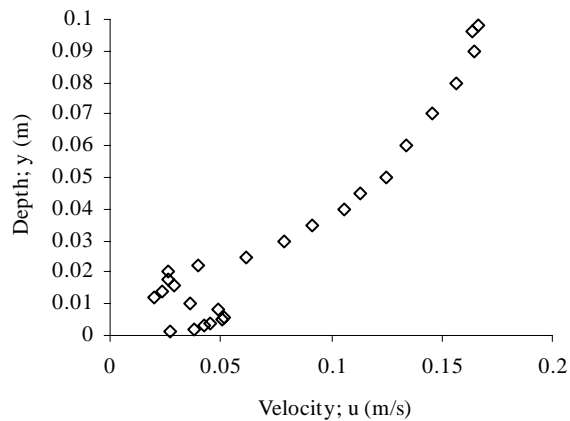


Figure 3. Velocity profile with under-mat flow

4 CONCLUSIONS

In this paper the traditional logarithmic velocity equation (Eq. 1) has been modified to account for a virtual bottom occurring in the flow-field within geosynthetic erosion control mats. This was achieved using an effective base height, k_g , resulting in the modified log-law of Equation 2. This was seen to fit the experimental profiles well. The presence of a bare geomat affects the flow-field by reducing the flow velocity of the fluid gradually through the depth of the mat. This enforces a compensatory increase in the flow velocities in the remaining flow.

Equation 2 has the same form as the ‘canopy flow’ equations (Jackson 1981, Thom 1971) used in meteorology which describes wind flow profiles occurring in the atmospheric boundary layer through vegetation canopies (e.g. forests, crops, etc.). This has led the authors to the conclusion that the hydraulic flow over and through a geomat produces a micro-canopy flow phenomenon. This conclusion is supported by the data collected, during the testing, at a location where a geomat was not properly secured to the flume base allowing the mat to rise of the base level (Fig.3).

Figure 3 shows a profile similar to that produced in micro-meteorological studies of forest where, within the bare trunk region, the lack of foliage cover allows for an increase of local flow velocities. It is important to be aware of this phenomenon as it means that if a mat is not securely placed, seepage flow below the mat will occur leading to the possibility of erosion and the failure of the system in question.

The work discussed above, shows that the modified log law equation holds for the conditions of the testing completed to date and the authors feel confident that, with more testing, a theoretical framework could be developed for the determination of velocities over specific geomats. This, it is hoped, will in itself lead to a better understanding of the properties of erosion control geotextiles.

REFERENCES

- Chow, V.T. 1973. *Open-channel hydraulics*. Singapore: McGraw-Hill.
- Garde, R.J., Ranga Raju, K.J. 1977. *Mechanics of Sediment Transport and Alluvial Stream Problems*. New Delhi: Wiley Eastern Press.
- Jackson, P.S. 1981. On the displacement height in the logarithmic velocity profile. *J. Fluid Mechanics*, 111: 15-25
- Keogh, D.P., Addison, P.S. 1996. Coherent flow structures in open-channel slot flow, *Coherent flow structures*, Ashworth, P.J., Bennett, S.J., Best, J.L., McLelland, S.J. (Editors), 14: 267-280. Chichester: John Wiley and Sons.

- McKay, D., Hytiris, N., Addison, P.S. 1998. Studies of Erosion Control Geomat Using Laser Doppler Anemometry, *Proc. VII Int. Symp. on River Sedimentation*: 337-342. Rotterdam: A.A.Balkema,.
- Nezu, I., Nakagawa, H. 1993. *Turbulence in Open-Channel Flows*. Rotterdam: A.A. Balkema.
- Nezu, I., Rodi, W. 1986. Open Channel Flow Measurements with a Laser Doppler Anemometer, *ASCE J. Hydraulic Eng.* 112: 115-119.
- Yalin, M.S. 1972. *Mechanics of Sediment Transport*. Braunschweig: Pergamon Press.